Research Letter

INTERNATIONAL JOURNAL OF SURGERY

OPEN

Clinical performance of a machine learning-based model for detecting lymph node metastasis in papillary thyroid carcinoma: A multicenter study

Wei Liu, MD[a,#], Jiaojiao Zheng, MD[a,#], Liang Han, MD[b,#], Weifeng Qu, MD[a], Qiao Wu, MD[a], Zhou Yuan, MD[c], Gaolei Jia, MD[d], Xiaolong Wang, MD[e], Linxiong Ye, MSc[f], Jiaqi Zhang, MSc[f], Shisheng Zhang, PhD[f], Xuanye Cao, PhD[f,*], Ying Liu, MD[g,h,i,*], Zhilong Ai, MD, PhD[a,*]

Abstract

Papillary thyroid carcinoma (PTC) is a common endocrine malignancy with a generally favorable prognosis, but lymph node metastasis (LNM) complicates treatment and increases recurrence risk. Current preoperative methods like neck ultrasound often miss LNM, leading to unnecessary surgeries. This study developed a non-invasive, artificial intelligence (AI)-driven predictive model for LNM using gene expression data from 157 PTC patients and validated it with qRT-PCR across 807 participants from multiple centers. The model focused on three key genes – RPS4Y1, PKHD1L1, and CRABP1 – chosen for their predictive strength. A random forest algorithm achieved high accuracy, with an AUROC of 0.992 in training and 0.911–0.953 in external validation. RPS4Y1 emerged as a standout predictor, showing the strongest distinction between metastatic and non-metastatic cases. The study also identified immune-related pathways, such as TGF-β signaling and cancer-associated fibroblast activation, as critical in metastasis. This gene expression-based model offers a non-invasive, cost-effective solution for predicting LNM, providing valuable insights to guide surgical decisions and reduce unnecessary procedures, ultimately improving patient outcomes.

Keywords: machine learning, precision oncology, PTC metastasis

[a]*Department of General Surgery (Thyroid & Breast), Zhongshan Hospital, Fudan University, Shanghai, China,* [b]*Department of Head and Neck Surgery, Tumor Hospital Affiliated to Nantong University, Nantong, Jiangsu, China,* [c]*Department of General Surgery, Sixth People's Hospital Affiliated to Shanghai Jiao Tong University School of Medicine, Shanghai, China,* [d]*Department of Thyroid surgery, Xuzhou Central Hospital, Xuzhou, China,* [e]*Department of General Surgery, Xuhui Central Hospital, Shanghai, China,* [f]*Department of Biological Medicines & Shanghai Engineering Research Center of Immunotherapeutics, School of Pharmacy, Fudan University, Shanghai, China,* [g]*Department of Engineering Research Center, Southeast University–Affiliated Xuzhou Central Hospital, Jiangsu, China,* [h]*Jiangsu Provincial Engineering Research Center of Cancer Cell Therapy and Translational Medicine, Xuzhou City Engineering Research Center of Cancer Cell Therapy and Translational Medicine, Jiangsu, China, and* [i]*School of Life Sciences, Jiangsu Normal University, Xuzhou, Jiangsu, China*

[#]*These authors have contributed equally to this work and share their first authorship*

**Corresponding Author. Address: Department of General Surgery (Thyroid & Breast), Zhongshan Hospital, Fudan University, Shanghai 200032, China. E-mail: aizhilong@126.com (Z. Ai); Department of Biological Medicines & Shanghai Engineering Research Center of Immunotherapeutics, School of Pharmacy, Fudan University, Shanghai, China. (X. Cao); School of Life Sciences, Jiangsu Normal University, Xuzhou, Jiangsu, China. (Y. Liu).*

International Journal of Surgery (2025) 111:4062–4067

Received 26 March 2025; Accepted 03 April 2025

Supplemental Digital Content is available for this article. Direct URL citations are provided in the HTML and PDF versions of this article on the journal's website, www.lww.com/international-journal-of-surgery.

Published online 22 April 2025

http://dx.doi.org/10.1097/JS9.0000000000002400

Background

Thyroid cancer, one of the most prevalent endocrine malignancies, has experienced a significant global rise in incidence[1,2]. Papillary thyroid carcinoma (PTC), which accounts for approximately 90% of all thyroid cancers, is categorized as a well-differentiated subtype[1,3]. Although PTC typically carries favorable prognosis, it frequently presents with lymph node metastasis (LNM), complicating surgical treatment and increasing the risk of recurrence[3,4]. Central LNM in PTC is reported to occur in 30–65% of cases, while lateral LNM is observed in approximately 20–30%, with more aggressive disease reaching as high as 50%[5-8].

Preoperative LNM assessment primarily depends on neck ultrasound, but its diagnostic accuracy is limited, particularly for central cervical LNM. Studies have shown that central and lateral metastases are either misreported or overlooked in 78.6% and 42.3% of cases, respectively, prompting surgical management changes based on surgeon-performed ultrasound in 65.4% of patients[9]. This diagnostic uncertainty often leads to unnecessary fine needle aspiration and prophylactic lymph node dissection in suspected cases[4,10]. Thus, an accurate, non-invasive, and efficient preoperative method for predicting LNM is urgently needed.

This study aims to combine genomic data with advanced artificial intelligence (AI) algorithms to develop a predictive model for LNM based on gene expression profiles in primary thyroid tumors. This approach could greatly enhance preoperative LNM risk assessment, leading to more precise surgical planning, fewer unnecessary lymph node dissections, and

HIGHLIGHTS

- Developed an artificial intelligence-driven model for predicting lymph node metastasis (LNM) in papillary thyroid carcinoma (PTC) using gene expression data from 157 patients, validated with qRT-PCR across 807 participants.
- Focused on three predictive genes – RPS4Y1, PKHD1L1, and CRABP1 – demonstrating strong predictive strength for LNM.
- The random forest algorithm achieved an AUROC of 0.992 in training and 0.911–0.953 in external validation, indicating robust predictive performance.
- Identified critical immune-related pathways, including TGF-β signaling, associated with metastasis, highlighting the role of immune response in tumor progression.
- The gene expression-based model offers a cost-effective, non-invasive solution for LNM prediction, aiding surgical decision-making and potentially reducing unnecessary procedures.
- Acknowledged the necessity for more diverse cohorts and additional validation of key predictors to establish their causality and enhance model robustness across different populations.

a reduced risk of recurrence and secondary surgeries, ultimately improving patient outcomes.

Methods

The detailed experimental procedures are provided in the Supplementary Methods (Supplementary File 1, available at: http://links.lww.com/MS9/A803).

Transcription profiling and marker discovery for metastatic PTC

To investigate transcriptional changes during PTC metastasis, RNA-seq was performed on tumor tissues from 157 PTC patients, including 107 metastatic and 50 primary cases. Differential expression analysis identified 180 upregulated and 236 downregulated genes in metastatic PTC (Figure S1A, available at: http://links.lww.com/MS9/A804). MSigDB Hallmark analysis highlighted TGF-β signaling and estrogen response pathways, both associated with tumor invasion (Figure S1B and 1C, available at: http://links.lww.com/MS9/A804). Downregulated genes were enriched in immune-related pathways such as cytokine-cytokine receptor interaction, aligning with the enhanced mobility of metastatic cells (Figure S1D and 1E, available at: http://links.lww.com/MS9/A804). MCP-Counter analysis further revealed a significant reduction in B lineage cells in metastatic PTC, indicating impaired immune responses (Figure S1F, available at: http://links.lww.com/MS9/A804).

To identify diagnostic markers for LNM, 40 marker genes were selected from the identified DEGs using the Boruta feature selection method based on the random forest models trained on the 157 PTC patients. The final trained random forest model based on the selected genes achieved a strong area under the curve (AUC) of 0.923 (95% CI: 0.880–0.966) with 80.4% sensitivity (95% CI: 71.9–86.8%) and 90.0% specificity (95% CI: 78.6–95.7%) (Figure S1G and 1H, available at: http://links.lww.com/MS9/A804). Further analysis using RNA-seq data from the TCGA-THCA (Thyroid carcinoma) cohort compared 185 PTC patients with LNM and 102 primary PTC, identifying 152 upregulated and 332 downregulated genes (Figure S2A, available at: http://links.lww.com/MS9/A804). The Boruta method identified 33 marker genes from the identified DEGs to train another random forest model, achieving an AUC of 0.802 (95% CI: 0.751–0.853) (Figure S2B and 2C, available at: http://links.lww.com/MS9/A804). Despite some variation between the Chinese cohort and TCGA data, four genes – RPS4Y1, PKHD1L1, CRABP1, and RBP4 – were shared, demonstrating their diagnostic potential across populations (Figure S2D, available at: http://links.lww.com/MS9/A804).

Due to the limitations of conventional qRT-PCR, which allows for testing only three markers simultaneously, RPS4Y1, PKHD1L1, and CRABP1 were selected for downstream qPCR validation. These genes were prioritized based on their high predictive value, excellent primer and probe specificity, and strong signal intensity, making them optimal candidates for reliable and precise testing. To further investigate the association between three genes and clinical characteristics of the patients, gene expression levels were categorized as high or low based on the median value and assessed with Chi-square tests. Overall, CRABP1 and PKHD1L1 were significantly associated with T stage and lymph node detection, while RPS4Y1 was significantly associated with age, T stage, vital status, and gender. No significant associations were found for race (Table S1, available at: http://links.lww.com/MS9/A805). GSEA analysis revealed that high CRABP1 expression enriched hormone signaling, thyroid hormone synthesis, and vascular smooth muscle contraction (Figure S3A, available at: http://links.lww.com/MS9/A804); elevated PKHD1L1 expression enriched B cell receptor signaling, hormone signaling, TRP channel regulation, and thyroid hormone synthesis (Figure S3B, available at: http://links.lww.com/MS9/A804); and high RPS4Y1 expression enriched amino acid biosynthesis, cell cycle, DNA replication, IL-17, and NF-κB signaling pathways (Figure S3C, available at: http://links.lww.com/MS9/A804).

Algorithm development and clinical validation

The predictive performance of five machine learning models was evaluated across three independent datasets (Nantong, Zhongshan, and Xuzhou) to assess their effectiveness in predicting thyroid cancer metastasis. The overall study workflow is illustrated in Fig. 1, consisting of two main phases: algorithm development and clinical validation. In the algorithm development phase, 458 participants from the Nantong dataset were used for model training and testing, with hyperparameter tuning performed through 5-fold cross-validation to optimize performance. In the clinical validation phase, 366 participants from Zhongshan and Xuzhou datasets were initially considered, with 349 undergoing qPCR testing. After applying exclusion criteria, 339 cases were included in the final analysis. The cohort was stratified into non-metastasis (n = 185) and metastasis (n = 154) groups for primary analysis. Additionally, among the metastasis cases, 24 participants had recorded location data, enabling a secondary analysis of central compartment (n = 17) and

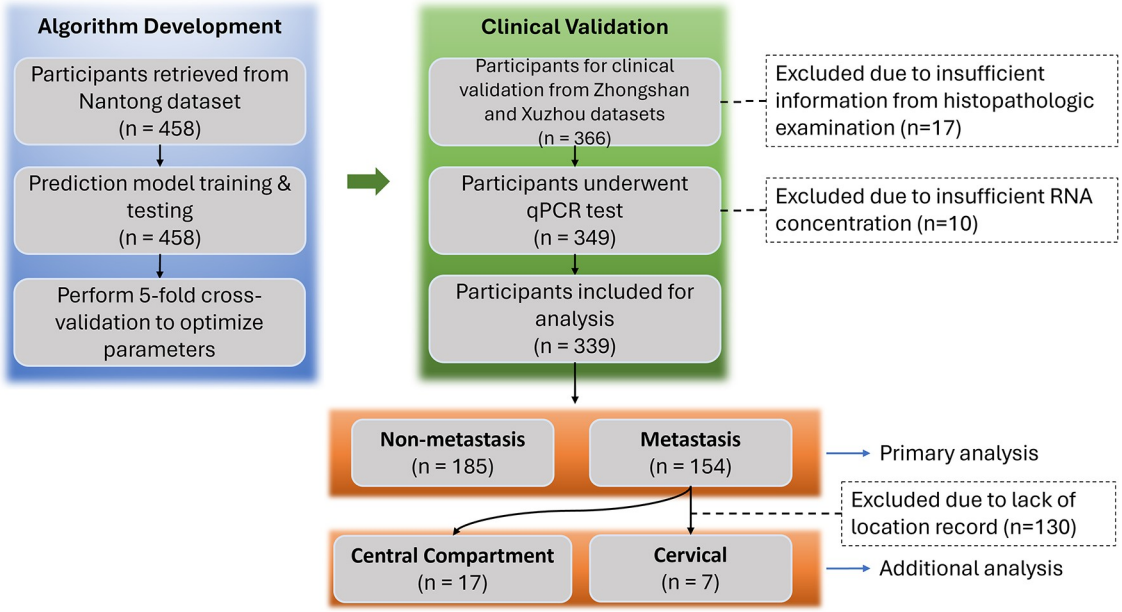

Figure 1. Flowchart showing the algorithm development and clinical validation process for predicting thyroid cancer metastasis. In the Algorithm Development phase, 458 participants from the Nantong dataset were used for prediction model training and testing, with 5-fold cross-validation applied to optimize parameters. In the Clinical Validation phase, 366 participants from the Zhongshan and Xuzhou datasets were considered, with 349 undergoing qPCR testing. A total of 339 participants were included in the final analysis, with exclusions due to insufficient histopathologic information (n = 17) and insufficient RNA concentration (n = 10). The cohort was divided into non-metastasis (n = 185) and metastasis (n = 154) groups, with 24 participants further analyzed for central compartment (n = 17) and cervical (n = 7) metastasis location. Additionally, 130 participants were excluded due to a lack of location record.

cervical metastasis (n = 7). A total of 130 cases were excluded from the location-based analysis due to missing records. As summarized in Table S2 (available at: http://links.lww.com/MS9/A805), the random forest model consistently outperformed the other algorithms across all datasets. In the Nantong dataset, random forest achieved the highest scores, with an accuracy of 0.949, precision of 0.896, recall of 0.976, F1-score of 0.934, and an AUROC of 0.992. Similarly, the Zhongshan and Xuzhou datasets demonstrated robust performance, with random forest achieving accuracies of 0.894 and 0.886, and AUROCs of 0.911 and 0.953, respectively. In contrast, logistic regression and deep learning models generally underperformed, particularly in recall and AUROC metrics, across all three datasets.

To explore the role of PKHD1L1, RPS4Y1, and CRABP1 in metastasis, their ΔCT values were analyzed across three datasets (Fig. 2A), revealing significant differences between metastatic and non-metastatic cases, with RPS4Y1 showing the most distinct separation. ROC curves (Fig. 2B) demonstrated strong predictive performance of the random forest model, achieving AUCs of 0.992 (Nantong), 0.953 (Xuzhou), and 0.911 (Zhongshan). Confusion matrices (Fig. 2C–E) confirmed high classification accuracy: Nantong achieved 271 true negatives and 164 true positives, Zhongshan identified 17 true negatives and 34 true positives, and Xuzhou classified 151 non-metastasis and 99 metastasis cases with minimal errors.

The performance of four machine learning models was also assessed using the Nantong and Zhongshan datasets to predict the location of thyroid cancer metastasis (central compartment vs. cervical). Random forest consistently outperformed the other models (Table S3, available at: http://links.lww.com/MS9/A805), achieving an accuracy of 0.952, precision of 0.891, recall of 1.000, F1-score of 0.942, and an AUROC of 0.991 in the Nantong dataset. While XGBoost performed well, it did not surpass random forest in any metric. In the Zhongshan dataset, random forest's accuracy dropped to 0.833 with an AUROC of 0.870, reflecting decreased performance compared to Nantong. This decline may be attributed to differences in patient demographics, clinical practices, or technical variations in sample processing across different institutions. Further investigation is needed to determine the extent to which these factors impact model performance and to explore potential strategies for improving generalizability across clinical settings. Figure 2F shows the ΔCT value distributions of PKHD1L1, RPS4Y1, and CRABP1 in central and cervical metastasis groups, highlighting distinct expression differences across both datasets. ROC curves (Fig. 2G) demonstrate our model's strong performance, with an AUC of 0.991 in Nantong but a lower AUC of 0.870 in Zhongshan. Confusion matrices (Fig. 2H, 2I) further illustrate the model's performance. These results demonstrate our model's superior accuracy and consistency across different clinical settings, establishing it as a robust tool for metastasis prediction, though its predictive power may vary depending on the clinical environment. To further understand the model's decision-making process, we analyzed feature contributions using SHAP values (Fig. 2J, 2K). The SHAP summary plots illustrate the importance and directional impact of key features on metastasis and location predictions. The color gradient highlights how high or low feature values influence predictions. Higher SHAP values indicate a stronger positive impact on the model's output, increasing the likelihood of the predicted outcome, whereas more negative SHAP values suggest a protective effect, reducing

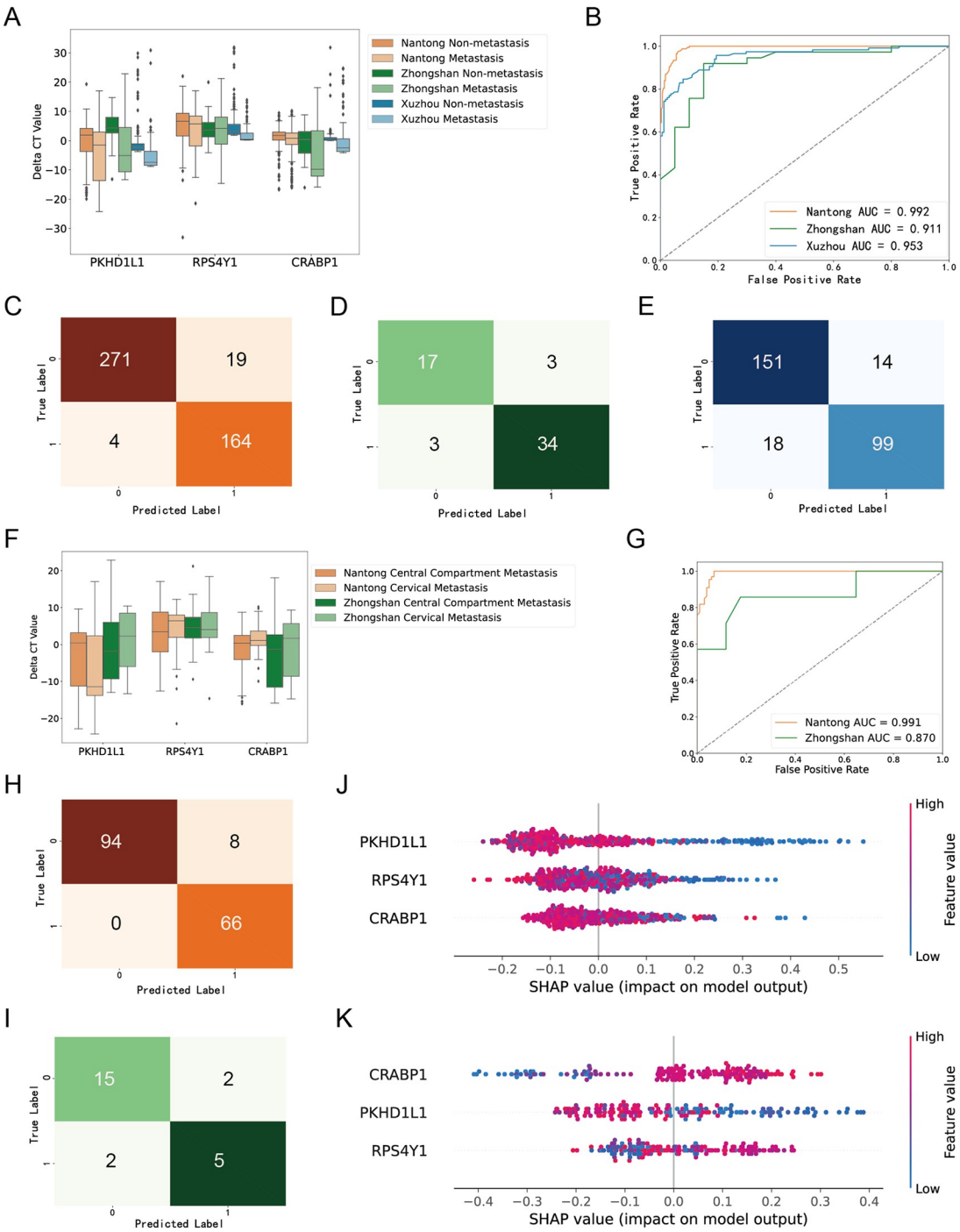

Figure 2. Performance of random forest in predicting thyroid cancer metastasis occurrence on multiple datasets. (A) Boxplots showing the distribution of ΔCT values for three genes (PKHD1L1, RPS4Y1, and CRABP1) across the Nantong, Zhongshan, and Xuzhou datasets, categorized into metastasis and non-metastasis groups. An asterisk (*) is added above two boxes if the statistical test shows a significant difference ($P < 0.05$). (B) Receiver operating characteristic (ROC) curves for metastasis prediction across the three datasets, with respective area under the curve (AUC) values: Nantong (0.992), Zhongshan (0.911), and Xuzhou (0.953). (C–E) Confusion matrices demonstrating the performance of random forest on the Nantong, Zhongshan, and Xuzhou datasets, respectively, for metastasis prediction. (F) Boxplots showing the distribution of ΔCT values for three genes (PKHD1L1, RPS4Y1, and CRABP1) across the Nantong and Zhongshan datasets, categorized into central compartment and cervical metastasis groups. An asterisk (*) is added above two boxes if the statistical test shows a significant difference ($P < 0.05$). (G) Receiver operating characteristic (ROC) curves for central compartment and cervical metastasis prediction, with respective AUC values: Nantong (0.991) and Zhongshan (0.870). (H and I) Confusion matrices demonstrating random forest performance on the Nantong (H) and Zhongshan (I) datasets for predicting metastasis location. (J and K) display the importance ranking and impact of different features on the model's output. Each dot represents a sample, with SHAP values indicating the contribution of each feature to the prediction. Positive SHAP values suggest a higher likelihood of the predicted outcome. The color gradient represents feature values, where red denotes higher values and blue denotes lower values. In metastasis prediction (J), PKHD1L1 was identified as the most important feature, while in location prediction (K), CRABP1 had the highest impact.

the probability of metastasis. In the metastasis prediction task (Fig. 2J), higher expression of PKHD1L1, RPS4Y1, and CRABP1 was associated with more negative SHAP values, suggesting that these genes may have a protective role against metastasis. In the location prediction task (Fig. 2K), these features also played a significant role, but their impact varied, indicating a distinct biological mechanisms underlying metastasis and tumor localization.

For metastasis prediction (non-metastasis vs. metastasis), we performed 5-fold cross-validation using the Nantong dataset, obtaining a Brier score of 0.0651 on each held-out fold. The Brier score measures both the accuracy and calibration of probabilistic predictions, where lower values indicate better-calibrated predictions. The relatively low Brier score in cross-validation suggests that the model performs well in predicting metastasis within the Nantong dataset. To assess the model's generalizability, we evaluated its performance on two external test datasets. The Brier scores for Zhongshan (0.1654) and Xuzhou (0.1444) were higher than those from the cross-validation results, indicating some degree of performance degradation when applied to unseen data. This suggests potential domain shifts or differences in patient populations across datasets, which may affect the model's calibration and reliability in external settings. For location prediction (central compartment vs. cervical), we conducted 5-fold cross-validation on the Nantong dataset, achieving a Brier score of 0.0544, indicating well-calibrated predictions within the training distribution. When tested on the Zhongshan dataset, the Brier score increased to 0.1332, reflecting a decline in predictive calibration. This performance drop highlights dataset variability and potential challenges in generalizing across different clinical cohorts.

Discussion

Accurate LNM prediction is essential for effective patient management, especially given the limitations of ultrasound (US) in certain anatomical regions. Central LNM detection *via* US is particularly challenging due to anatomical constraints and the absence of typical LNM features such as microcalcifications and increased vascularity[4,11]. To overcome these limitations, machine learning (ML) has shown great promise as a tool for predictive modeling in various biomedical fields[12,13]. ML and radiomics have emerged as promising alternatives for improving LNM prediction. For instance, Liu *et al* utilized radiomics to predict LNM by extracting 614 features from B-mode ultrasound images and developed a support vector machine model that achieved an AUC of 0.78 on the training set and 0.73 on the test set[14]. Similarly, Chang *et al* designed a nomogram incorporating deep learning, clinical data, and US features, with AUCs ranging from 0.809 to 0.829 in the validation cohort[15]. A recent meta-analysis reported pooled AUCs of 0.84 for radiomics-only models and 0.81 for models combining radiomics with clinical data, suggesting that the inclusion of clinical data does not significantly enhance diagnostic performance[16]. However, in multicenter and cross-machine applications, the performance of both clinical and traditional radiomics models decreased substantially. Independent tests revealed AUCs of 0.67 and 0.56 for models based solely on clinical information and traditional radiomics, respectively[3]. These findings underscore the need for more robust and reproducible diagnostic tools to improve LNM prediction.

Our findings suggest that RPS4Y1, CRABP1, and PKHD1L1 play critical roles in LNM prediction. While RPS4Y1 remains underexplored, CRABP1 and PKHD1L1 have established associations with PTC and metastasis. CRABP1, involved in retinoid signaling, is significantly downregulated in PTC, promoting epithelial-mesenchymal transition via the epidermal growth factor receptor pathway and contributing to tumor invasiveness[17,18]. Its downregulation, often due to promoter hypermethylation, has been linked to increased LNM risk[19]. Similarly, PKHD1L1 acts as a potential tumor suppressor in thyroid cancer, with reduced expression correlating with larger tumor size, distant metastasis, and advanced disease stage[20,21]. It has also been implicated in immune cell infiltration, suggesting a role in the tumor microenvironment[22,23]. Our pathway analysis further supports immune-related alterations in metastatic PTC, reinforcing the biological relevance of these genes in LNM prediction.

Despite promising results, limitations remain. Although our study used multi-center data from hospitals in China, the cohort is predominantly Chinese. This may limit the model's generalizability to other ethnic groups or regions. Further validation in diverse populations is needed to assess its broader applicability. Core predictors like RPS4Y1, CRABP1, and PKHD1L1 require further validation to establish causality. Additionally, relying solely on gene expression may overlook factors like post-transcriptional modifications and protein interactions that impact metastasis.

Conclusions

In conclusion, this study highlights the potential of integrating gene expression profiles with AI models to predict LNM in PTC accurately. Key gene markers provide insights into metastasis mechanisms, and the externally validated model offers a non-invasive, cost-effective tool for preoperative risk assessment, enhancing surgical decisions and minimizing unnecessary interventions. Future studies with larger, more diverse populations and further validation of these markers will be crucial to maximize the model's clinical impact.

Ethical approval

None.

Consent

None.

Sources of funding

This research was supported by Shanghai Innovation Medical Device Application Demonstration Project 2023:23SHS05200. Y.J.Z. was supported by Zhongshan Hospital Foundation of Youth Fund 2022ZSQN15.

Author contributions

Z.A. and Y.L. designed the research and analyzed the data. W. L., J.Z., J.H., Q.W., W.Q., G.J., and X.C. performed research

and analyzed data. W.L. wrote the paper. Z.A., Z.Y., L.Y., S.Z., J.Z., and Y.L. revised the manuscript critically for important intellectual content. All authors contributed to the article and approved the submitted version.

Conflicts of interest disclosure

The authors declare no potential conflicts of interest.

Research registration unique identifying number (UIN)

None.

Guarantor

Zhilong Ai.

Provenance and peer review

Not commissioned, externally peer-reviewed.

Data availability statement

The datasets analyzed in the current study are available upon request from the corresponding author.

Acknowledgments

We appreciate the assistance received in data processing and consultation from Villanelle Life (Shanghai) Co. Ltd.

References

[1] Boucai L, Zafereo M, Cabanillas ME. Thyroid cancer: a review. Jama 2024;331:425–35.
[2] Siegel RL, Miller KD, Wagle NS, Jemal A. Cancer statistics, 2023. CA Cancer J Clin 2023;73:17–48.
[3] Yu J, Deng Y, Liu T, *et al*. Lymph node metastasis prediction of papillary thyroid carcinoma based on transfer learning radiomics. Nat Commun 2020;11:4807.
[4] Haugen BR, Alexander EK, Bible KC, *et al*. 2015 American Thyroid Association management guidelines for adult patients with thyroid nodules and differentiated thyroid cancer: the American Thyroid Association guidelines task force on thyroid nodules and differentiated thyroid cancer. Thyroid 2016;26:1–133.
[5] Mao J, Zhang Q, Zhang H, Zheng K, Wang R, Wang G. Risk factors for lymph node metastasis in papillary thyroid carcinoma: a systematic review and meta-analysis. Front Endocrinol (Lausanne) 2020;11:265.
[6] Qiao D, Deng X, Liang R, *et al*. Nomogram to predict central lymph node metastasis in papillary thyroid carcinoma. Clin Exp Metastasis 2024;41:613–26.
[7] Roh JL, Kim JM, Park CI. Central lymph node metastasis of unilateral papillary thyroid carcinoma: patterns and factors predictive of nodal metastasis, morbidity, and recurrence. Ann Surg Oncol 2011;18:2245–50.
[8] Sun W, Lan X, Zhang H, *et al*. Risk factors for central lymph node metastasis in CN0 papillary thyroid carcinoma: a systematic review and meta-analysis. PLoS One 2015;10:e0139021.
[9] Tapia M, Chia C, Manji J, Magarey MJR, Flatman S. Surgeon-performed ultrasound changes surgical management in patients with thyroid cancer. ANZ J Surg 2022;92:3268–72.
[10] Nixon IJ, Ganly I, Patel SG, *et al*. Observation of clinically negative central compartment lymph nodes in papillary thyroid carcinoma. Surgery 2013;154:1166–73.
[11] Hwang HS, Orloff LA. Efficacy of preoperative neck ultrasound in the detection of cervical lymph node metastasis from thyroid cancer. Laryngoscope 2011;121:487–91.
[12] Fang YAO, Xia FEI, Tian F, *et al*. Machine learning and bioinformatics to identify biomarkers in response to Burkholderia pseudomallei infection in mice. Biocell 2024;48:613–21.
[13] Wang Y, Wang M, Yu K, *et al*. A machine learning model to predict efficacy of neoadjuvant therapy in breast cancer based on dynamic changes in systemic immunity. Cancer Biol Med 2023;20:218–28.
[14] Liu T, Zhou S, Yu J, *et al*. Prediction of lymph node metastasis in patients with papillary thyroid carcinoma: a radiomics method based on preoperative ultrasound images. Technol Cancer Res Treat 2019;18:1533033819831713.
[15] Chang L, Zhang Y, Zhu J, *et al*. An integrated nomogram combining deep learning, clinical characteristics and ultrasound features for predicting central lymph node metastasis in papillary thyroid cancer: a multicenter study. Front Endocrinol (Lausanne) 2023;14:964074.
[16] HajiEsmailPoor Z, Kargar Z, Tabnak P. Radiomics diagnostic performance in predicting lymph node metastasis of papillary thyroid carcinoma: a systematic review and meta-analysis. Eur J Radiol 2023;168:111129.
[17] Hsu YC, Huang WC, Kuo CY, Li YS, Cheng SP. Downregulation of cellular retinoic acid binding protein 1 fosters epithelial-mesenchymal transition in thyroid cancer. Mol Carcinog 2023;62:1935–46.
[18] Celestino R, Nome T, Pestana A, *et al*. CRABP1, C1QL1 and LCN2 are biomarkers of differentiated thyroid carcinoma, and predict extrathyroidal extension. BMC Cancer 2018;18:68.
[19] Huang Y, de la Chapelle A, Pellegata NS. Hypermethylation, but not LOH, is associated with the low expression of MT1G and CRABP1 in papillary thyroid carcinoma. Int J Cancer 2003;104:735–44.
[20] Wang QX, Chen ED, Cai YF, *et al*. A panel of four genes accurately differentiates benign from malignant thyroid nodules. J Exp Clin Cancer Res 2016;35:169.
[21] Zheng C, Quan R, Xia EJ, Bhandari A, Zhang X. Original tumour suppressor gene polycystic kidney and hepatic disease 1-like 1 is associated with thyroid cancer cell progression. Oncol Lett 2019;18:3227–35.
[22] Hogan MC, Griffin MD, Rossetti S, Torres VE, Ward CJ, Harris PC. PKHDL1, a homolog of the autosomal recessive polycystic kidney disease gene, encodes a receptor with inducible T lymphocyte expression. Hum Mol Genet 2003;12:685–98.
[23] Liao Z, Cheng Y, Zhang H, *et al*. A novel prognostic signature and immune microenvironment characteristics associated with disulfidptosis in papillary thyroid carcinoma based on single-cell RNA sequencing. Front Cell Dev Biol 2023;11:1308352.